

# Rabi oscillations of solitons in spin-chains: a new route to quantum computation and communication

S. Bertaina,<sup>1,2,\*</sup> C-E. Dutoit,<sup>1</sup> J. Van Tol,<sup>3</sup> M. Dressel,<sup>4</sup> B. Barbara,<sup>5,6</sup> and A. Stepanov<sup>1</sup>

<sup>1</sup>*Aix-Marseille Université, CNRS, IM2NP UMR7334, 13397 cedex 20, Marseille, France.*

<sup>2</sup>*TGE Réseau National de RPE interdisciplinaire, FR-3443.*

<sup>3</sup>*Physics Department and the National High Magnetic Field Laboratory, Florida State University, 1800 E. Paul Dirac Drive, Tallahassee, Florida 32310*

<sup>4</sup>*Physikalisches Institut, Universität Stuttgart, 70550 Stuttgart, Germany*

<sup>5</sup>*Univ. Grenoble Alpes, Inst. NEEL, F-38042 Grenoble, France.*

<sup>6</sup>*CNRS, Inst. NEEL, F-38042 Grenoble, France.*

(Dated: Submitted)

Most of qubit systems known to date are isolated paramagnetic centres in magnetically diluted samples since their dilution allows to considerably weaken the dipole-dipole inter-qubit interaction and thus to prevent the decoherence. Here we suggest an alternative approach for spin qubits which are built on spin  $S = 1/2$  defects in magnetically concentrated strongly correlated systems - spin chains. The corresponding qubits are made of spin solitons resulting from local breaking of transitional symmetry associated with point-defects. We provide the first evidence for coherence and Rabi oscillations of spin solitons in isotropic Heisenberg chains, simple antiferromagnetic-Néel or spin-Peierls, proving that they can be manipulated as single spin  $S = 1/2$ . The entanglement of these many-body soliton states over macroscopic distances along chains, gives rise to networks of coupled qubits which could easily be decoupled at will in extensions of this work.

PACS numbers: 71.27.+a, 03.67.-a, 75.10.Pq, 76.30.-v

Most physical, chemical or biological systems showing quantum oscillations are of relatively small size: isolated NV-centers in diamond [1], 4f or 3d transition-metal ions (single-spins, 0.1 nm) [2, 3], single molecule magnets [4] (15 spins, 1 nm), or marine algae (5 nm wide proteins) [5]. Their environmental couplings are necessarily weak in order to reduce damping [6]. In magnetic systems, decoherence is usually dominated by spin-bath dipole-dipole interactions [7] and observations of quantum oscillations require *qubits dilution*. Here, we demonstrate the feasibility of a new approach for magnetic qubits, which relies on spin  $S = 1/2$  defects in *magnetically concentrated* strongly correlated systems - spin chains.

Following the idea of Loss-DiVincenzo spin-qubit quantum computer [8], an increasing number of proposals were made during the last decades showing theoretically how spin chains may enable the implementation of a quantum computer. Most of them discuss the possibility of using spin chains as quantum wires to connect distant qubits registers without resorting to optics [9–14]. Different versions of Heisenberg model were considered with the purpose to see how the entanglement between two distant spins depends on magnetic anisotropy [11], temperature [10, 11, 15], applied magnetic field [10, 11], frustration [13, 15] and lattice dimerization [13]. It was concluded that, in spite of short-ranged spin correlations, most spin-chain models exhibit the long-distance entanglement [10, 12, 15], thus a spin chain can be used as a communication channel. However, according to this scheme, to realize a qubit network one needs first to create qubits and then to match them to the communication channels.

Therefore, we suggest to built up a qubit network without adding any new spins to the chain, but by using topological defects of a spin chain called solitons (or kinks) as qubits. Solitons are frequently viewed as a mobile domain walls representing by a large number of correlated spin. In a presence of crystallographic defects/disorder (bond-alternation defects, chain ends etc.) the solitons are trapped by the defect [16] and since they carry a spin  $S = 1/2$  they can serve as a qubit (hereafter, we will consider only this type of qubits and we will call them soliton-qubits (sol-qubits)).

From what has been said, theoretically, it appears that a spin chain itself represent a very promising network for solid state quantum information processing.

From experimental side, however, the situation is less clear. While there are some experimental indications that the macroscopic entanglement can be achieved in spin systems [14], almost nothing is known about quantum dynamics of sol-qubits. Moreover, the general experimental situation concerning the coherent dynamics of magnetic cluster, nanomagnets, rings etc rather indicates that the decoherence time in these objects is very short thus preventing their use as qubits.

In this Letter we present the first and clear evidence of long-living Rabi oscillations in sol-qubits with the decoherence time up to a several  $\mu s$ , which show exceptional figures of merit larger than 20 and are extremely robust against microwave decoherence. These results open the way to further prospects and practical applications of spin chains in quantum information processing.

This first study of sol-qubits was performed on single-crystals of the so-called antiferromagnetic quantum spin

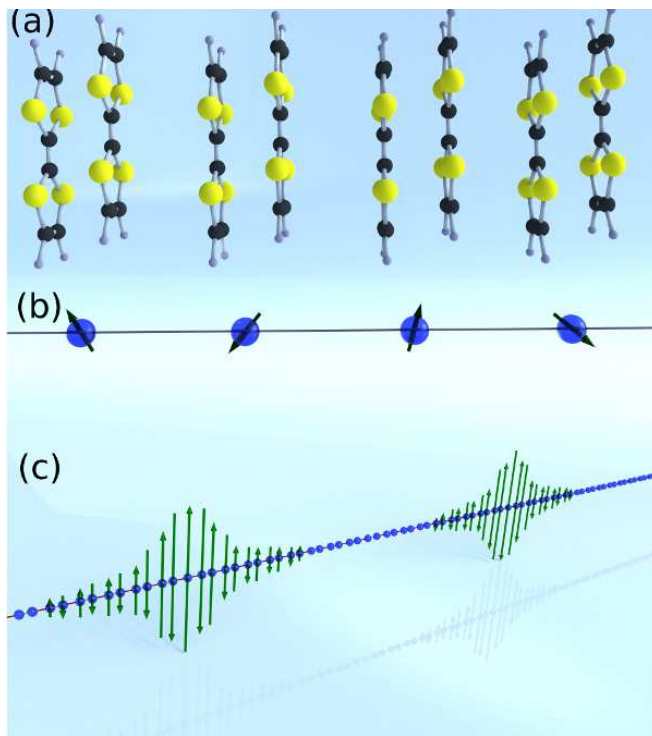


FIG. 1. Colour online. (a) Schematic representation of (TMTTF)<sub>2</sub>X chain. The TMTTF molecules are stacked in the *a* axis direction forming the chain. Each double molecules of TMTTF carries a spin  $S = 1/2$ . The counter anion X is not represented here. (b), magnetic representation of the chain. The blue spheres are the double molecules of TMTTF carrying a spin (black arrow) and coupled along the *a* axis by the exchange  $J(1 \pm \delta)$ . (c), artistic view of trapped solitons in a dimerized spin chain. Here the defect is a non-dimerized spin which polarized the neighbor sites. The green arrows are the local magnetization. The global shape of the soliton is inspired by DMRG simulation.

chains (TMTTF)<sub>2</sub>X, with X = AsF<sub>6</sub>, PF<sub>6</sub>, SbF<sub>6</sub> (Fig. 1). This family of organic magnets, also called Fabre salts [17], was extensively studied during the last decades and shows an extremely rich phase diagram [18]. The physical properties of these magnets depend on the counter anion X of the molecule and are found to be quite sensitive on the presence of paramagnetic defects (spin-Peierls and superconducting transition). The systems with X = AsF<sub>6</sub> and PF<sub>6</sub> show a gapped dimerized spin-pair singlet ground-state below their spin-Peierls transitions at  $T_{SP} = 13$  K and 19 K respectively, whereas the system with X = SbF<sub>6</sub> exhibits a Néel antiferromagnetic phase below  $T_N = 7$  K.

The isotropic part of the exchange interaction of these three systems,  $J \sim 400$  K, is relatively large whereas the intra- and inter-dimer contributions of (TMTTF)<sub>2</sub>PF<sub>6</sub> and (TMTTF)<sub>2</sub>AsF<sub>6</sub>, give a bond alternation (dimerization) parameter  $\delta \sim 0.03$  leading to the singlet-triplet gap  $\Delta = 35$  K [19]. Such a value is more than enough to

provide an excellent separation of the ground state at the Kelvin scale of temperatures, i.e. an extended collective singlet ground-state in which two trapped soliton qubits can be strongly entangled.

The single crystals of (TMTTF)<sub>2</sub>X were grown by an electrochemical technique. The crystals are needle-shaped with typical dimensions:  $3 \times 0.5 \times 0.1$  mm<sup>3</sup>. The samples crystallize in the triclinic  $P\bar{1}$  space group. The magnetic principal axes ( $b'$  and  $c^*$ ) are different from the crystallographic axes [20]. The static magnetic field can be applied in any direction in the  $b'-c^*$  plane. For each set of measurements a fresh sample was used.

Continuous Wave (CW) and Pulsed Electron Paramagnetic Resonance experiments were performed with the three systems using a conventional X-band Bruker spectrometer operating at about 9.7 GHz between 3 K and 300 K and enabling sample rotations. The crystals were glued on the sample holder with their *a*-axis oriented along the microwave field ( $h_{mw}$ ) direction which is the same as the sample-rotation direction (the static  $H$  being applied in the basal  $b'-c^*$  plane).

Above 30 K a single Lorentzian-shaped EPR line (main line) is observed, displaying an anisotropy of  $g$  factor, associated with different orientations of  $H$ , and its temperature dependence which are typical of uniform quantum Heisenberg spin chains. Below about 30 K a second EPR line, a very sharp one, appears in the three systems at the same magnetic field as the main line. The integrated intensity of this sharp signal is much smaller (by a factor of  $10^2 - 10^3$ ) than the one of the main line, indicating its defect origin.

As an example, figure 2(a) gives a set of spectra obtained with X = AsF<sub>6</sub> between 30 K and 3 K with  $H \parallel c^*$  showing how the very sharp signal progressively appears below 30 K. Below  $T_{SP} = 13$  K the system starts to dimerise and enters in the spin-Peierls phase. The intensity of the main peak drops but that of the sharp peak remains almost unchanged. The same behaviour has been observed in PF<sub>6</sub> compound. In the SbF<sub>6</sub> system, the linewidth of the main line diverges when  $T$  decreases down to  $T_N = 7$  K whereas the sharp-line remains unchanged, except below  $T_N$  where it disappears [21]. This behaviour is quite contrary to that of an isolated paramagnetic impurity, the intensity of which is strongly temperature-dependent (Curie law), and is rather characteristic of an ensemble of correlated spins.

In the limit of the resolution of the X-band spectrometer, the measured resonance field and therefore the  $g$  factor were identical for both the broad and sharp peaks and did not change significantly for different molecules. A two-lorentzian fit shows that their linewidths differ by a factor of ten ( $\sim 1$  G for the former and  $\sim 0.1$  G for the latter, Fig. 2(b)). In order to improve the resolution we measured the CW-EPR in these systems at 120 GHz in a homemade quasi-optical CW-EPR spectrometer [22] (the angular dependence of the magnetic field

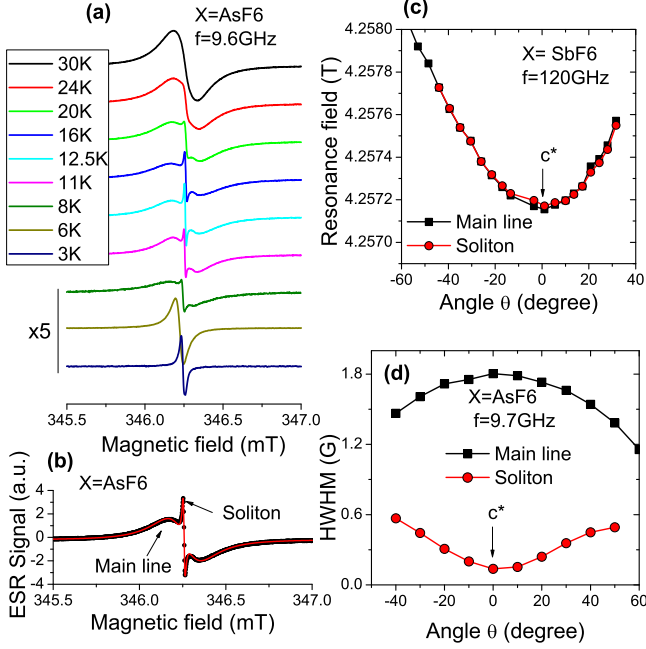


FIG. 2. color online. CW-EPR, evidence of the soliton signal. (a) Set of CW-EPR spectra of (TMTTF)<sub>2</sub>AsF<sub>6</sub> when the temperature decreases for  $H \parallel c^*$ . (b) EPR spectrum of (TMTTF)<sub>2</sub>AsF<sub>6</sub> at  $T = 12.5$  K. The dots are the experiments and the red line is a fit of 2 derivative of Lorentzian. (c) Angular dependence of the resonance fields of (TMTTF)<sub>2</sub>SbF<sub>6</sub> at 120 GHz. The black squares are the main lines, the red circles are the soliton lines. (d) Angular dependence of the linewidth of (TMTTF)<sub>2</sub>AsF<sub>6</sub> at 9.5 GHz and  $T = 12.5$  K.

resonance of the SbF<sub>6</sub> system is given in figure 2(c). The resonance fields of both lines remaining identical for all the applied-field orientations to an accuracy better than  $10^{-5}$ .

Figure 2(d) gives the linewidth angular dependence of the two peaks observed. The broad/sharp linewidth ratio reaches its maximum of  $\sim 10$  when the static field is applied along the  $c^*$  axis. Surprisingly, whereas the resonant field of the two peaks is observed to be the same whatever the angle  $\theta$ , the angular dependences of their linewidths are opposite. The width of the broad line follows the well-known behavior of a uniform  $S = 1/2$  chain (proportional to  $1 + \cos^2 \theta$ , with a maximum for  $\theta = 0^\circ$ ) whereas the one of the sharp line is minimum for  $\theta = 0^\circ$ . This last result indicates that the linewidth-angular dependence of a semi-infinite spin chain is fundamentally different from that of a large but finite number of correlated spins (soliton). To sum up, all our EPR findings and model analysis clearly show that the observed sharp signal stems from the correlated spin-chain defects bears a spin  $S = 1/2$ , which we attribute to trapped solitons.

The pulsed EPR experiments were performed on (TMTTF)<sub>2</sub>AsF<sub>6</sub> and (TMTTF)<sub>2</sub>PF<sub>6</sub> single crystals with a microwave field  $h_{mw}$  varying between 0.1 and 1.5 mT.

The coherent signal, resulting from the sharp EPR line observed in CW experiments, was recorded by the Free Induction Decay method. The spin-echo detection cannot be used here, in contrast with most other known systems, because of the absence of sizable inhomogeneous line-broadening. In fact the line-broadening of  $\sim 0.1$  G observed is essentially homogeneous (see discussion below). Examples of Rabi oscillations obtained at 3 K for  $X = \text{PF}_6$  are given in figure 3. The oscillations are very well-fitted by the exponentially damped sinusoidal function  $\langle S_x(t) \rangle \propto \sin(\Omega_R t) \exp(-t/\tau_R)$  with  $\Omega_R$  the Rabi pulsation and  $\tau_R$  the Rabi damping characteristic time. The Rabi frequency increases linearly with  $h_{mw}$  with a slope  $d(\Omega_R/2\pi)/dh_{mw} \sim 28$  MHz/mT close to the expected value for spins  $S = 1/2$  (Fig. 3(b)), thus providing an additional evidence in favour of our model of a trapped soliton with  $S = 1/2$ .

This figure also shows the microwave-field dependence of the Rabi damping  $1/\tau_R$  allowing one to evaluate the damping by the microwaves, the same as those which induce the Rabi oscillations [2, 4, 23]. This “over-damping”, associated with inhomogeneous line-broadening due to distributions of the transverse  $g$  factor (resulting itself from weak ligand-field distributions) or to the microwave-field amplitude (non-homogeneous cavities) is generally unavoidable [24]. In the present case, and this is rather exceptional, the “over-damping” is particularly small due to the homogeneous character of the EPR line. The measured value of  $d(1/\tau_R)/dh_{mw} = 0.4$  MHz/mT (Fig. 3(b)), is 10 to 50 times smaller than in ion diluted systems [23, 24]. In addition, contrary to most other systems, the figure of merit  $Q_M = \Omega_R \tau_R / 2\pi$  of sol-qubits in (TMTTF)<sub>2</sub>PF<sub>6</sub> does not saturate when the Rabi frequency increases (Fig. 3(c)) and follows the expression  $Q_M = \Omega_R / (8.5 + 0.015\Omega_R)$ . Our largest microwave field  $h_{mw} = 1.5$  mT gives at 3 K  $Q_M \sim 23$  while a value of the order of 70 may be expected for a larger field. Whereas  $Q_M$  of CaWO<sub>4</sub>:Er<sup>3+</sup> and MgO:Mn<sup>2+</sup> which saturate at about 3,  $Q_M$  of sol-qubits is an order of magnitude larger.

The fact that sol-qubits are almost not sensitive to system parameters ( $g$  factors, inhomogeneous magnetic and microwave fields, etc.) is worthy of special consideration. Qubits are actually never identical and in most qubit systems they are coupled by the *magnetic dipole-dipole interaction* which is inevitably a major source of decoherence. In the present case the situation is just opposite: the interactions between qubits eliminate the decoherence caused by inhomogeneous distributions of Rabi frequencies. The reason is that we deal here with an ensemble of  $S = 1/2$  defects (sol-qubits) in a strongly correlated spin-chain system. In consequence, the dynamics of two sol-qubits even distant from each other is not independent but controlled by an effective *isotropic exchange* interaction. We anticipate that the physical picture developed for the interacting  $S = 1/2$  degrees of

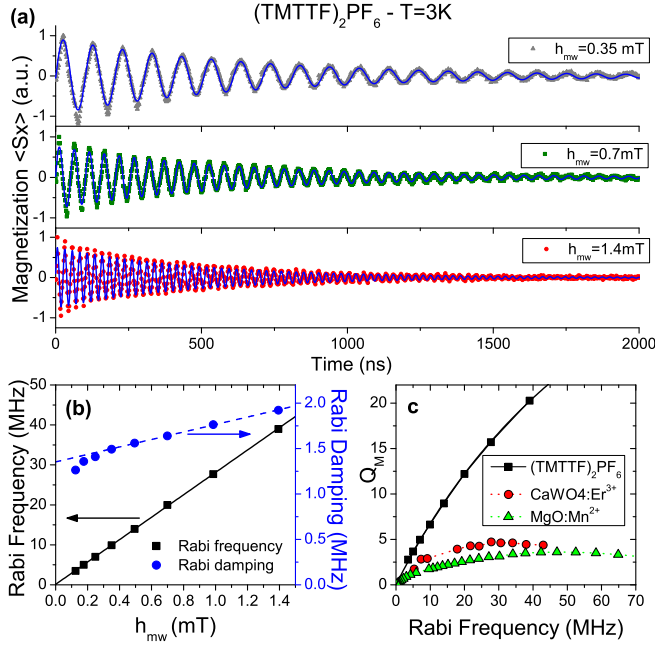


FIG. 3. colour online. Rabi oscillations and coherence properties of soliton-qubit. (a) Series of Rabi oscillations of  $(\text{TMTTF})_2\text{PF}_6$  measured at  $T = 3\text{ K}$  and  $f = 9.7\text{ GHz}$  using the FID method while increasing the microwave magnetic field  $h_{mw}$ . Each point is an average of 1000 FID measurements. The blue lines are fits using  $\sin(\Omega_R) \cdot \exp(t/\tau_R)$ . (b) Rabi frequencies ( $\Omega_R/2\pi$ ) and damping ( $1/\tau_R$ ) as function of  $h_{mw}$ . The black line represents the Rabi frequency of spin  $S=1/2$ . The blue line is a fit using  $\Gamma_0 + \gamma \cdot h_{mw}$ ,  $\Gamma_0 = 1.35\text{ MHz}$  (the zeros microwave field coherence) and  $\gamma = 0.41\text{ MHz/mT}$  the effect of microwave field on the Rabi damping. (c) Merit factor  $Q_M$  of  $(\text{TMTTF})_2\text{PF}_6$  compared to diluted ion systems [24]. The black line is a simulation using the  $\Gamma_0$  and  $\gamma$  from (b).

freedom in Haldane spin chains with  $S = 1$  can be applied here [25]. This leads to a kind of narrowing mechanism which homogenizes the parameter distributions explaining why the coherence of sol-qubits, rather robust against microwaves, is limited by  $2T_2^*$ .

In conclusion, we suggest that  $S = 1/2$  defects in strongly correlated spin-chain systems can be used for quantum information processing. This is in striking contrast with known spin-qubits systems where qubits are uncoupled or weakly coupled by an anisotropic interaction leading to decoherence. By observing long-living Rabi oscillations of sol-qubits in Heisenberg gapped spin-Peierls systems, we provide first and clear evidence for the coherence of solitons trapped at defects in spin-chains. Due to an isotropic inter-qubit exchange interaction, the EPR lines observed are homogeneous and narrowed. This eliminates most of the decoherence mechanisms associated with disorder i.e. with non-perfectly identical qubits. Remarkably, the important effect of decoherence by the microwaves which tends to burst out

with the number of qubits is shown to be here negligible. In the present case, coherent spin-information is not transferred by tractable inter-dots semiconducting-insulating tunnel-barrier [8], but by simple addressing spin-chains singlet-portions which fulfill the required conditions for the implementation of a quantum computer. These results obtained at a zero moment transfer ( $q \sim 0$ , as in most EPR experiments) may be extended to the case of finite  $q$  in which case the response would not be limited to trapped sol-qubits but also to travelling sol-qubits, implying an instantaneous spin-state transfer or teleportation from one end of the chain to another one (non-locality) using spin-chains as quantum wires to connect distant qubits registers without resorting to optics [26]. This work constitutes the first stone paving the way for the very exciting physics of coherent dynamics of spin-chains solitons, either frozen (sol-qubit quantum computers) or moving (teleportation, quantum communication through singlet spin-channels, dynamical coherent spin-transport etc.).

We acknowledge the city of Marseille, Aix Marseille Université, NHMFL user program for financial support. We thank G. Gerbaud and PFM St Charles for technical support. SB and BB thank I. Chiorescu and S. Miyashita for valuable discussions.

---

\* sylvain.bertaina@im2np.fr

---

\* sylvain.bertaina@im2np.fr

- [1] L. Childress, M. V. Gurudev Dutt, J. M. Taylor, A. S. Zibrov, F. Jelezko, J. Wrachtrup, P. R. Hemmer, and M. D. Lukin, *Science* **314**, 281 (2006).
- [2] S. Bertaina, S. Gambarelli, A. Tkachuk, I. N. Kurkin, B. Z. Malkin, A. Stepanov, and B. Barbara, *Nat. Nanotechnol.* **2**, 39 (2007), arXiv:0703364.
- [3] S. Bertaina, L. Chen, N. Groll, J. Van Tol, N. S. Dalal, and I. Chiorescu, *Phys. Rev. Lett.* **102**, 50501 (2009), arXiv:0812.4534.
- [4] S. Bertaina, S. Gambarelli, T. Mitra, B. Tsukerblat, A. Müller, and B. Barbara, *Nature* **453**, 203 (2008).
- [5] E. Collini, C. Y. Wong, K. E. Wilk, P. M. G. Curmi, P. Brumer, and G. D. Scholes, *Nature* **463**, 644 (2010).
- [6] A. Leggett, S. Chakravarty, A. Dorsey, M. Fisher, A. Garg, and W. Zwerger, *Reviews of Modern Physics* **59**, 1 (1987).
- [7] N. V. Prokof'ev and P. C. E. Stamp, *Rep. Prog. Phys.* **63**, 669 (2000).
- [8] D. Loss and D. P. DiVincenzo, *Phys. Rev. A* **57**, 120 (1998).
- [9] W. K. Wootters, *Phys. Rev. Lett.* **80**, 2245 (1998).
- [10] M. Arnesen, S. Bose, and V. Vedral, *Phys. Rev. Lett.* **87**, 017901 (2001).
- [11] G. Lagmago Kamta and A. Starace, *Phys. Rev. Lett.*



- 88**, 107901 (2002).
- [12] S. Bose, Phys. Rev. Lett. **91**, 207901 (2003).
  - [13] L. Campos Venuti, C. Degli Esposti Boschi, and M. Roncaglia, Phys. Rev. Lett. **96**, 247206 (2006).
  - [14] L. Amico, A. Osterloh, and V. Vedral, Reviews of Modern Physics **80**, 517 (2008).
  - [15] L. Campos Venuti, C. Degli Esposti Boschi, and M. Roncaglia, Phys. Rev. Lett. **99**, 060401 (2007).
  - [16] D. Khomskii and M. Mostovoy, Zeitschrift für Physik B Condensed Matter **103**, 209 (1997).
  - [17] J. Moser, M. Gabay, P. Auban-Senzier, D. Jérôme, K. Bechgaard, and J. Fabre, The European Physical Journal B **1**, 39 (1998).
  - [18] D. Jérôme, Science (New York, N.Y.) **252**, 1509 (1991).
  - [19] M. Dumm, B. Salameh, M. Abaker, L. K. Montgomery, and M. Dressel, Journal de Physique IV (Proceedings) **114**, 57 (2004).
  - [20] S. Yasin, B. Salameh, E. Rose, M. Dumm, H.-a. Krug von Nidda, A. Loidl, M. Ozerov, G. Untereiner, L. Montgomery, and M. Dressel, Phys. Rev. B **85**, 1 (2012).
  - [21] C. Coulon and R. Clérac, Chem. Rev. **104**, 5655 (2004).
  - [22] J. van Tol, L.-C. Brunel, and R. J. Wylde, Rev. Sci. Instrum. **76**, 074101 (2005).
  - [23] J. Shim, S. Bertaina, S. Gambarelli, T. Mitra, A. Müller, E. Baibekov, B. Malkin, B. Tsukerblat, and B. Barbara, Phys. Rev. Lett. **109**, 1 (2012).
  - [24] H. De Raedt, B. Barbara, S. Miyashita, K. Michielsen, S. Bertaina, and S. Gambarelli, Phys. Rev. B **85**, 014408 (2012).
  - [25] P. Mitra, B. Halperin, and I. Affleck, Phys. Rev. B **45**, 5299 (1992).
  - [26] I. M. Pop, I. Protopopov, F. Lecocq, Z. Peng, B. Pannetier, O. Buisson, and W. Guichard, Nat. Phys. **6**, 589 (2010).